Article

Inequitable distribution of risks associated with occupational heat exposure driven by trade

Meng Li [1], Bo Meng [2,3] ✉, Yong Geng [1,4] ✉, Fan Tong [5,6,7], Yuning Gao [8], Norihiko Yamano [9], Sunghun Lim [10], Joaquim Guilhoto [11], Kimiko Uno [2,12] & Xiaohong Chen [13]

The exposure to extreme heat at workplaces poses substantial threat to human effort and manual labour. This becomes more prominent due to the global dispersion of labour-intensive production activities via trade. We combine a climate model with an input–output model to quantify the risks associated with trade-related occupational extreme heat exposure. Here we show an 89% surge in trade-related labour exposure to extreme heat, escalating from 221.5 to 419.0 billion person-hours between 1995 and 2020. Lower-middle-income and low-income economies constituted 53.7% and 18.3% of global exposure but only 5.7% and 1.0% of global labour compensation. In countries highly susceptible to extreme heat conditions, workers perform tasks in heated conditions for up to about 50% of their working hours. The disproportionate trade effects in redistributing global benefits and costs leads to the inequality in heat exposure between developed and developing economies. In striving for equitable and safe work conditions, workers vulnerable to heat extremes in developing economies should be protected by climate adaptation infrastructure, given their critical roles in the global production system.

Climate change has resulted in extreme heatwaves in more regions, where more populations are exposed to such adverse conditions[1–4]. Extreme temperature events have increased by 232% and caused 13% of all disaster deaths worldwide during the past two decades[5], which is a major risk to global sustainable development[6]. In particular, heatwaves caused over 70000 excess deaths in Europe during the summer of 2003 and over 55000 excess deaths in Russia in 2010[7,8]. To date, extreme heat waves have become a huge threat to the global labour force[9,10]. Billions of workers are exposed to unsafe heat, many of whom are working in the poorest and warmest regions[11]. Meanwhile, the rapid

development of global trade has led to the redistribution of both production and job opportunities[12,13]. Due to lower labour costs, labour in developing economies is encountering new job opportunities; however, they are also facing unprecedented risks associated with occupation heat exposure, especially those living in the most vulnerable regions[14]. Such exposure leads to significant adverse impacts, such as heightened health risks[15,16], increased mortality rates[17,18], and reduced labour productivity[19,20]. The exposure to extreme heat at workplaces poses a substantial threat to the achievement of Sustainable Development Goals (SDG), especially SDG8 (decent work and

[1]School of Environmental Science and Engineering, Shanghai Jiao Tong University, Shanghai, China. [2]Institute of Developing Economies, Japan External Trade Organization, Chiba, Japan. [3]Collaborative Innovation Center for Emissions Trading System Co-constructed by the Province and Ministry, Wuhan, China. [4]School of International and Public Affairs, Shanghai Jiao Tong University, Shanghai, P.R. China. [5]School of Economics and Management, Beihang University, Beijing, China. [6]Lab for Low-carbon Intelligent Governance, Beihang University, Beijing, China. [7]Peking University Ordos Research Institute of Energy, Ordos, China. [8]School of Public Policy and Management, Tsinghua University, Beijing, China. [9]The Organization for Economic Co-operation and Development, Paris, France. [10]Department of Agricultural Economics & Agribusiness, Baton Rouge, US. [11]International Monetary Fund, Washington D.C., US. [12]Gakushuin Women's College, Tokyo, Japan. [13]Hunan University of Technology and Business, Changsha, China. ✉e-mail: bo_meng@ide.go.jp; ygeng@sjtu.edu.cn

economic growth), SDG10 (reduced inequalities), and SDG13 (climate action).

Understanding the vulnerability of the global labour force to extreme heat is crucial for devising effective adaptation strategies. Existing studies have made significant progress in quantifying workplace heat exposure[9,21,22], estimating labour productivity and economic loss[23–26], measuring heat-related morbidity and mortality[27–30], and projecting future costs and losses based on various climate scenarios[31,32]. However, it is still unclear how international trade contributes to the distribution and extent of extreme heat exposure among the global labour force. From the production side, a country's vulnerability to extreme heat is shaped by its domestic production activities and its role in the international trade system[33], especially the climate risks faced by its labour force in producing traded goods[34]. From the consumption side, consumers should recognise the externalities of their demand, including the impact beyond local labour to foreign workers exposed to extreme heat challenges through international trade[35], to foster a more equitable understanding of the true costs of their consumption. This study aims to enrich the existing literature by uncovering the nexus between international trade and exposure to extreme heat among the global labour force.

We propose a comprehensive analytical framework that integrates a high-resolution global climate model[36], socio-economic and demographic information, and a global multi-regional input-output model to quantify the occupational extreme heat exposure among the labour force from 1995 to 2020 (Supplementary Figs. 1, 2). Using an extended multi-regional input-output model with a labour satellite account, we estimate labour employment embodied within the global production networks, which was downscaled to the grid level using gridded population datasets. High-resolution climate data enabled the identification of annual extreme heat hours for each grid cell. Incorporating country-specific working hours from the Penn World Table, we obtain the number of hours an average labourer was exposed to extreme heat at each grid cell per year. Linking labour embodied in production networks with extreme heat exposure, we quantify occupational heat exposure within the global production system with both spatial and temporal dimensions. We find that trade accounts for nearly one-quarter of the global labour force's total exposure to extreme heat, with a large flux of heat exposure transferred from developed economies to developing economies (Supplementary Table 1)[37]. These results indicate a high level of inequality between who causes climate change through historical emissions and who bears its negative consequences[38,39].

Results

Increasing heat exposure of labour force

Over the past three decades, heat exposure of the global labour force has increased substantially due to the changing climates[11,40], sustained long working hours[41], and increased international trade. The outsourced production via trade in labour-intensive sectors usually happens in countries with abundant labour force already subject to high ambient temperatures. Figure 1 illustrates the evolution of global heat exposure, categorised by production types—purely domestic production, where goods are produced and consumed within the same country, and via international trade, where goods are produced in one country and consumed in another[42]. The total heat exposure has surged by 60%, growing from 1142.3 billion person-hours in 1995 to 1826.2 billion person-hours in 2020. This equates to an annual rise of 27.3 billion person-hours, which would place such an increase among the top fifteen countries globally in terms of heat exposure if it were a country.

Trade-related exposure played a significant role, which increased from 221.5 billion person-hours to 419.0 billion person-hours during this study period (increased by 89%). Such rapid trade-related exposure growth has even outpaced the expansion in trade-related labour employment, with a 52% increase over this study period. The global average per capita working hours in heat-exposed conditions expanded from 485.6 h in 1995 to 578.1 h in 2020, meaning a substantial increase of 19.1%. To be more specific, the per capita exposed working hours for pure domestic production increased from 489.0 hours in 1995 to 575.4 hours in 2020, while such a figure for international trade increased from 471.7 hours in 1995 to 587.3 hours in 2020. The rapid increase in exposure per capita underscores the significant impact of climate change during the past three decades, potentially leading to even more severe risks associated with occupational heat exposure over this century under various Shared Socioeconomic Pathways (SSP) scenarios (Supplementary Figs. 3–6). Using the structural decomposition analysis (SDA)[43], we found that climate change, trade-related production structure, and trade-related final demand structure effect account for 102, 347, and 134 billion person-hours of the total increase (Supplementary Fig. 7).

Exposure to extreme heat is highly unequal, with production-side exposure more concentrated in developing economies. Trade plays disproportionate roles in redistributing global benefits and costs by generating more exposure than value-added or labour compensation (Fig. 2). In 1995, trade accounted for 18.9% of the global exposure, 19.9% of global labour employment, 13.8% of the global labour compensation, and 14.8% of the global value-added. However, the share of trade in the global labour compensation and value-added was still less
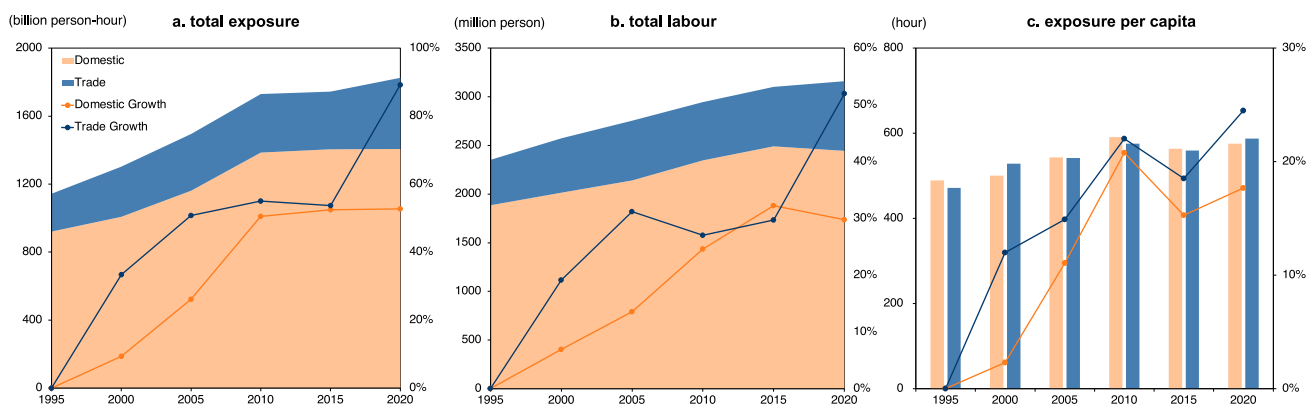
Fig. 1 | Global trends of labour and working hours exposed to heat stress.
a World's total exposure to heat stress classified by domestic production and international trade. The connected lines represent percentage change compared to the base year 1995. **b** World's total labour employment is classified by domestic production and international trade. The connected lines represent the percentage change compared to 1995. **c** The average annual exposure per capita for domestic production-related and trade-related workers. The connected lines represent the percentage change compared to 1995. Source data are provided as a Source Data file.
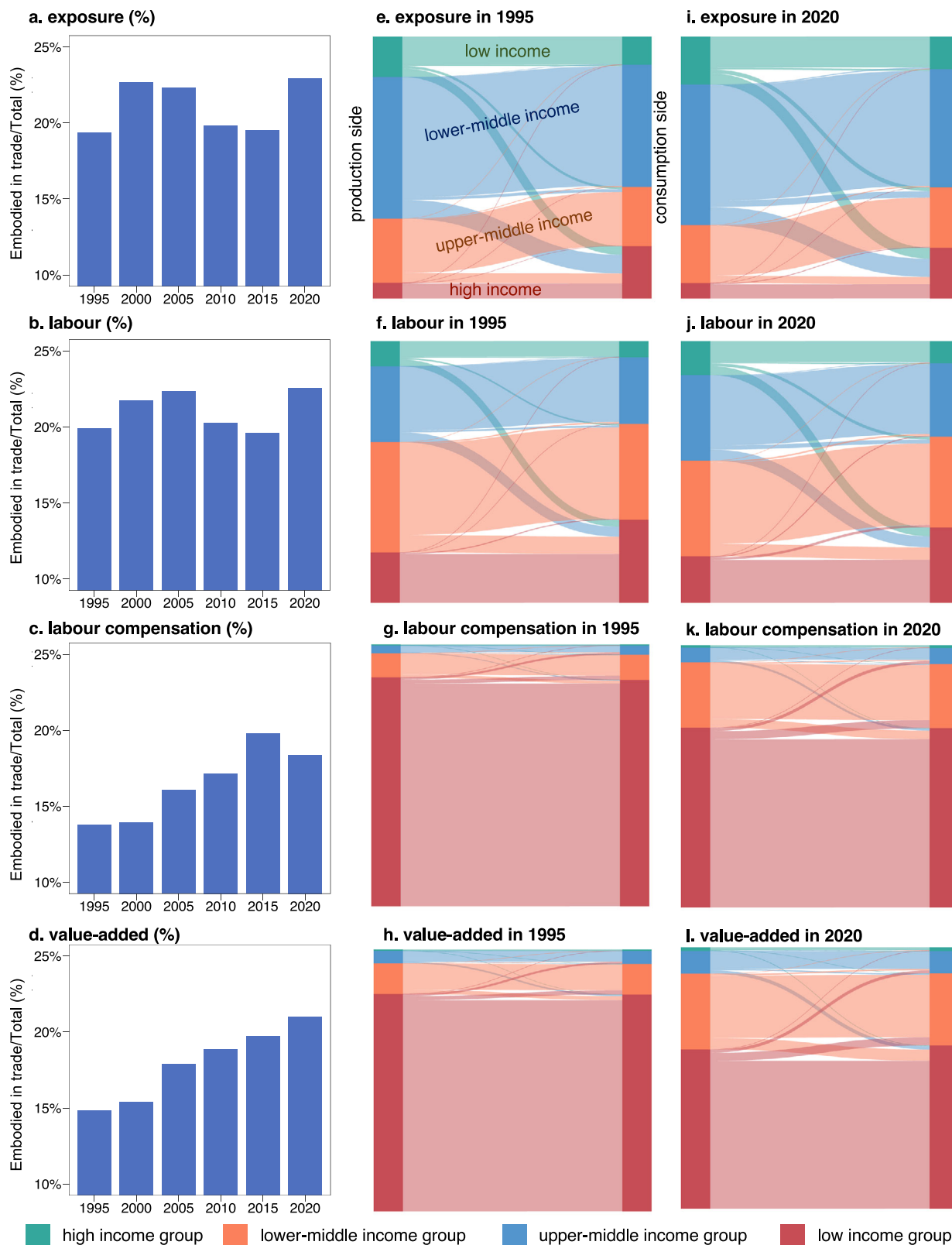
Fig. 2 | Unequal exchanges in labour, exposures, compensation, and value-added. a–d The share of (**a**) exposure, (**b**) labour employment, (**c**) labour compensation, and (**d**) value-added that is transferred embodied in trade compared to the global total value. **e–h** Global flows between high-income, upper-middle-income, lower-middle-income, and low-income economy groups in 1995 for (**e**) exposure, (**f**) labour employment, (**g**) labour compensation, and (**h**) value-added. **i–l** Global flows between high-income, upper-middle-income, lower-middle-income, and low-income economy groups in 2020 for (**i**) exposure, (**j**) labour employment, (**k**) labour compensation, and (**l**) value-added. Source data are provided as a Source Data file.

than that in the global exposure by the end of 2020. Following the World Bank's method for classifying economies based on Gross National Income (GNI) per capita[37], this study classifies all economies into four income groups: high-income, upper-middle-income, lower-middle-income, and low-income groups (Supplementary Table 1), with the latter three categories encompassing developing economies. Despite the changes in economic classification for some countries over time, this study abstracts from such shifts and uses a consistent categorisation to minimise bias associated with changes in group membership (Supplementary Table 1). This approach ensures that the analysis remains robust and comparable across different time periods. Figure 2e–l shows the inequitable exchange of heat exposure and socio-economic benefits between different income groups. The left side represents the production-based amount—the heat exposure borne by the labour within the territories and the right side represents the consumption-based amount—the relative footprint generated by their consumption of goods and services. From the production side, the high-income group accounted for an extremely small portion of global heat exposure (5.9%) and labour supply (17.8%) but a significantly larger share in global labour compensation (68.5%) and value-added (61.0%) in 2020. On the contrary, the lower-middle-income and low-income groups constituted the majority of global exposure (53.7% and 18.3%), and labour supply (32.6% and 13.0%), but their shares in global labour compensation (5.7% and 1.0%) and value-added (8.7% and 1.3%) were markedly low. Specifically, within the 5.9% of global exposure attributed to the production of high-income groups, 5.4% was for their own consumption and 0.5% was for exports. However, the goods and services they consumed resulted in 19.4% of the global total exposure. Of this, only 5.4% occurred within their own territories, with 2.8%, 7.0%, and 4.2% in upper-middle-income, lower-middle-income, and low-income groups, respectively. International trade has greatly improved global economic growth, but it is coupled with unequal resource, environmental and labour exchanges.

Huge exposure disparities across economies

Unequal exposure to extreme heat is stark across countries (Fig. 3 and Supplementary Figs. 8–15), with developing economies facing significantly higher exposure for their production activities (Supplementary Figs. 16, 17, 20). India, China, Indonesia, Nigeria, and Bangladesh were the top five countries in terms of total exposed hours in 2020, accounting for 24.7, 13.4, 7.3, 4.3, and 4.2% of the global total, respectively. These countries are labour-intensive, contributing to the global labour force with respective shares of 14.1, 22.8, 4.1, 2.0, and 2.1%, totalling 45.2%. In addition, they are highly susceptible to heat-exposed conditions. For instance, in Nigeria, an average worker might perform their tasks under heat stress for up to 1186.8 hours, or 59.4% of their working hours, during the year of 2020. Comparable figures for India, China, Indonesia, and Bangladesh are 47.6, 15.6, 50.8, and 48.4%, respectively. Wealthier economies (dark blue distributed on the left side) had fewer per capita working hours exposed to extreme heat compared to developing economies (light blue on the right side). High, upper-middle, lower-middle, and low-income economy groups were subject to 192.5, 348.5, 952.1, and 814.2 hours of heat exposure per capita. In particular, south-east Asia and Africa had the highest exposure rates. For instance, the average per capita exposed hours were 1319.5 in Thailand and 1186.8 in Nigeria in 2020, while the average per capita exposed hours were only 28.1 in Germany and 260.9 in the United States in 2020. More exposure hours in developing economies mean that those workers have to work longer under adverse climate conditions than their counterparts in developed economies.

Compared with production side exposure, the distribution of consumption side exposure is different as exposure is shifted from developing to developed economies (Supplementary Figs. 18, 19, 21). The consumption side exposure in the United States accounted for 6.2% of the global total exposure in 2020, which is nearly three times

their production side exposure (only 2.2%). The per capita exposure hours in high, upper-middle, lower-middle, and low-income economy groups were 389.0, 384.6, 931.3, and 847.0 h in 2020. In general, the consumption side exposure rate in the high-income group is twice as much as their production side exposure rate, indicating that they should take higher associated environmental costs.

The socio-economic characteristics play an essential role in such disparities, such as economic development level, industrial structure, average labour working hours, and trade patterns (Supplementary Fig. 22). Normally, a lower per capita Gross Domestic Product (GDP) is often related to a higher share of heavy work and longer annual per capita working hours, which all contribute to regional disparities. The per capita net exposure rate—measured as the difference between consumption-based exposure footprint and production-based exposure–is positive in wealthier economies, but negative in developing economies, indicating that developed economies have outsourced their environmental burdens (in this case, heat exposure) to developing economies via international trade. Such disparity is underscored by the significant differences in heat exposure per unit of value-added embodied in exports and imports across countries (Supplementary Figs. 23–28), highlighting the uneven distribution of costs borne by various labour forces engaging in global trade.

Trade redistributes global exposure

Figure 4 shows top exposure flows embodied in trade (Supplementary Fig. 29). Economies shaded in red have net exposure transferred to other places, such as those in North America and Europe; while economies shaded in blue have net exposure transferred from other places, such as those in South America, Africa, and Asia. The United States had the largest net exposure import embodied in trade from 2000 to 2020, from 29.2 billion person-hours in 1995 to 73.2 billion person-hours in 2020. China experienced a decrease in its net exposure export, from being the largest exporter (30.7 billion person-hours) in 1995 to only 0.3 billion person-hours in 2020. India was the largest net exposure exporter in 2020 (46.6 billion person-hours), followed by Vietnam, Indonesia, Bangladesh, and Ethiopia. During the past three decades, more developing economies have experienced an increase in their heat exposure, meaning that their workers have to take more public health consequences induced by climate change.

Exposure embodied in trade is closely related to the industrial structure in each economy. Figure 5a, b presents industry-specific exposure to extreme heat embodied in both exports and imports for the top twenty economies from 1995 to 2020 (Supplementary Fig. 30). The agriculture sector, characterised by labour-intensive activities conducted predominantly in non-sheltered settings, has a pivotal role in the global dispersal of vulnerability to extreme heat conditions. For instance, India recorded an alarming 59.8 billion person-hours of export-embodied exposure in 2020, of which 19.0 billion person-hours originated from its agricultural sector, accounting for 31.9% of its total exported exposure. The petroleum, chemical, and non-metallic mineral products and the retail sector followed this agriculture sector, but with figures of only 6.2 and 4.6 billion person-hours, respectively, which accounted for 10.4% and 7.7% of India's total export-embodied exposure.

Figure 5c, d illustrate the structural compositions of trade-embodied exposure, categorised by both sector and exporting/importing economy for 1995 and 2020, respectively. The agriculture sector was the dominated sector for trade-related exposure in 1995, with a figure of 121.9 billion person-hours and accounting for 55.0% of the global total, followed by both retail and wholesale sectors with figures of 9.7 and 9.2 billion person-hours and accounting for 4.4% and 4.2% of the global total. After three decades of globalisation, this agriculture sector remained its dominance, with a figure of 165.1 billion person-hours in 2020, but only accounting for 39.4% of the global total in 2020. Conversely, both retail and wholesale sectors increased their
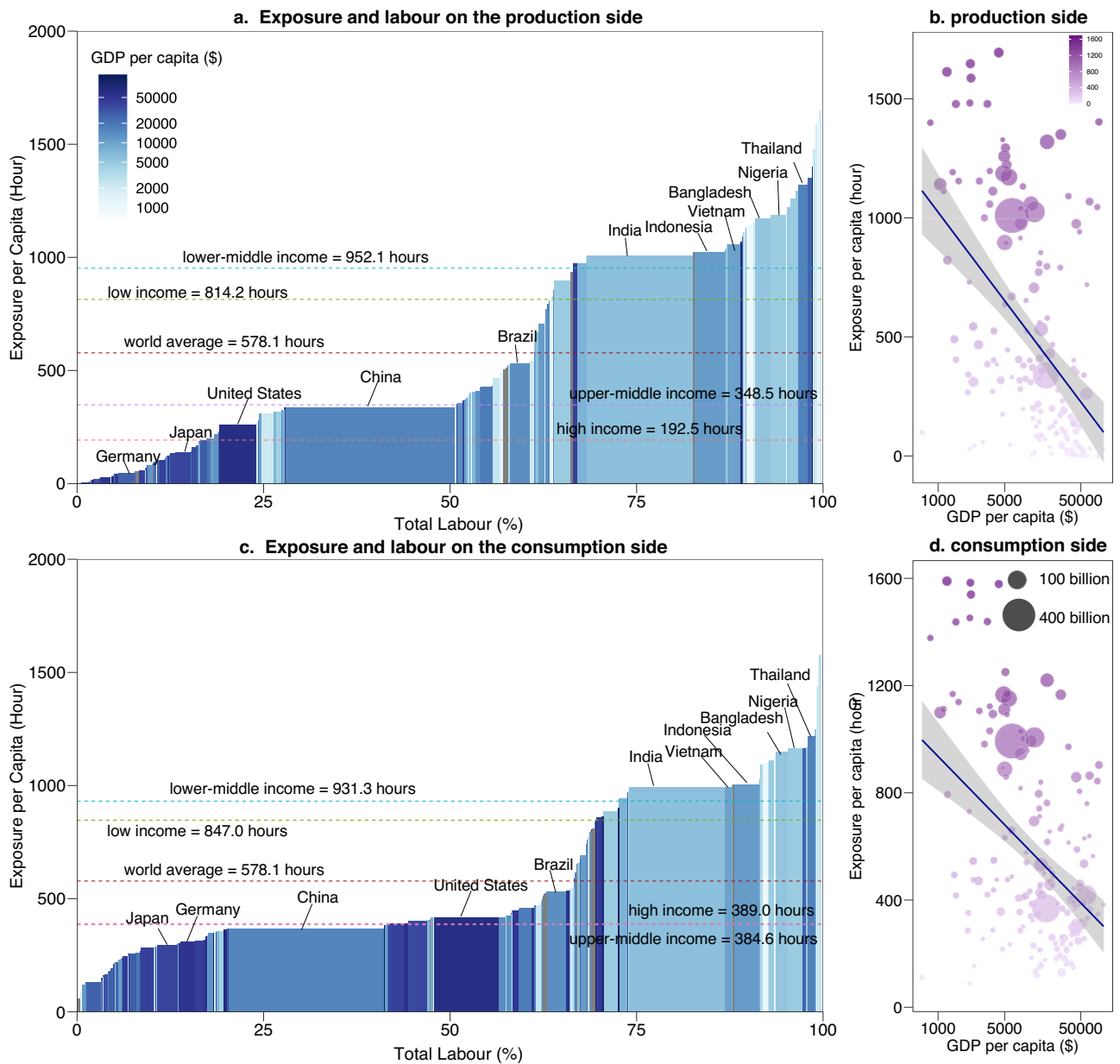
Fig. 3 | Working hour heat exposure in 2020 on both production and consumption sides. a, c Exposure rate per capita and their share in the global labour employment on (**a**) production side and (**c**) consumption side. **b, d** Negative relationship between exposure rate per capita and GDP per capita on (**b**) production side and (**d**) consumption side. All the per capita GDP values are purchasing-power-parity-based (constant 2017 international $). The size of the bubbles indicates the total heat exposure of the country's labour. The colour intensity of the bubbles represents the exposure per capita. The blue line represents the mean regression prediction, which estimates the expected exposure level for each value of GDP per capita. The shaded area indicates the 95% confidence interval around these mean predictions. Source data are provided as a Source Data file.

exposure hours, with figures of 28.92 and 28.21 billion person-hours, collectively contributing to 13.6% of the global total. China's agricultural sector, which was responsible for 6.4% of the global exposure trade in 1995—second only to India at 7.0%—experienced a significant decline to 1.7% in 2020 due to its gradual industrial transition toward manufacturing and services.

Discussion

In this study, we investigate the global exposure to extreme heat at work using an integrated framework combined with world climate derived from the fifth-generation European Centre for Medium-Range Weather Forecasts (ECMWF) reanalysis for the global climate and weather (ERA5), a multi-regional input-output model to link international production and consumption, as well as socioeconomic and demographic information (Supplementary Figs. 1, 2). Our study builds on previous studies on population-weighted heat exposure[44,45], to advance our understanding of the nexus between labour, trade, and climate change. The result that global trade has led to unequal labour heat exposure is consistent with the asymmetric effects of heat stress, where developing countries disproportionately suffer from health losses and labour productivity losses[33]. The results reveal a substantial human cost: in some countries, labour may work nearly half of their time under heat stress and such burden has increased by 89% globally. The rapidly increasing risks associated with occupational heat exposure align with the significant human cost of global warming—especially in countries like India, Indonesia, and Nigeria[46]—such as the nearly 200% stark increase in global urban exposure from 1983 to 2016[47] and the multifold population heat exposure in the rest of this century[40,48].
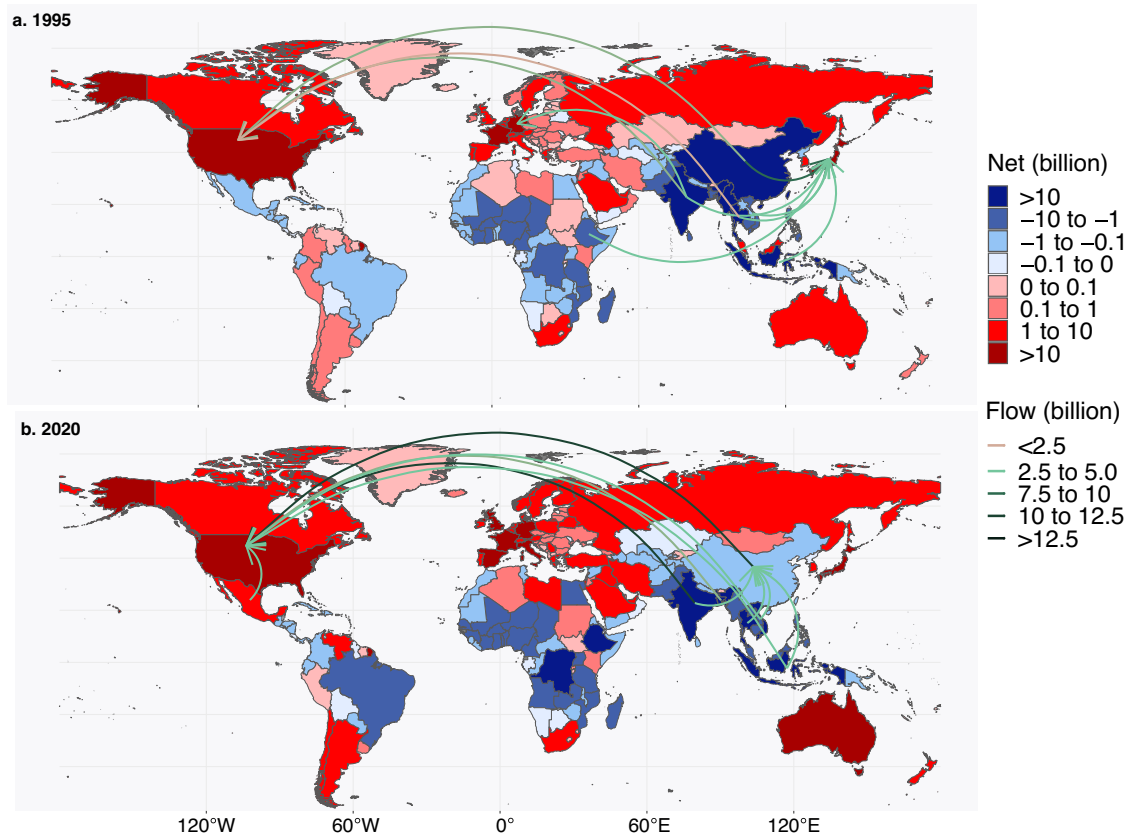
Fig. 4 | Top exposure flows embodied in trade. In (**a**) 1995 and (**b**) 2020, the filled colour represents the exposure balance measured by the difference between their consumption side exposure and production side exposure. Countries/regions filled in red have net exposure import (outsourcing to other places), while those filled in blue have net exposure export (original production place). These arrows represent the top ten exposure flows between different countries/regions, in which the colour and arrow width correspond to the size of each flow.

The results indicate an unequal burden of climate change, particularly across different countries, genders, and vulnerable groups[49]. Labour force in tropical and impoverished regions have to work under extreme heat conditions to struggle for a living, but neither their input nor their losses are adequately compensated[50–52]. The insufficient adaptation infrastructure further increased their risks and losses, especially for those most at-risk regions[53–56]. Without a concerted global effort, labour working in worse conditions may suffer from associated health risks, which may lead to reduced productivity of the global labour force. Gender also plays a crucial role in the unequal distribution of climate change effects[27]. In 2020, women's per capita working hours in heat-exposed conditions exceeded those of men (Supplementary Fig. 31). Women are particularly vulnerable due to their involvement in labour-intensive sectors, such as agriculture, Southeast Asian textile industries, and African artisanal mining. Social norms and gender wage gaps may limit women's access to adaptation resources, worsening their vulnerability to climate change. Also, despite SDG8 targets to end child labour in all its forms by 2025, there were 160 million children in child labour in 2020[57], constituting a substantial share of the global workforce and heat-exposed workers. The child labour—often in impoverished tropical regions—are especially vulnerable to heat exposure, bearing significant challenges to their health status and educational attainment. Moreover, the lack of governance in vulnerable countries may aggravate such risks[58,59]. Other factors, such as the lack of public awareness or backward medical conditions, further contribute to reduced labour productivity and increased economic losses[60,61], especially those engaging in labour-intensive tasks (Supplementary Figs. 31–34).

Economic instruments are essential for mitigating the risks faced by the labour force due to extreme heat. A primary policy should be the

collection and expansion of climate change funds, ensuring sufficient resources to assist developing economies and enhancing their climate adaptation infrastructure[62]. The disproportionate impact of climate change on developing economies necessitates a dedicated fund to compensate for climate-related losses and damages. To alleviate the financial burden, revenues from carbon pricing or tariffs could be allocated to reimburse the Loss and Damage funds to offset the costs of climate adaptation, mitigate the climate change losses, and internalise the environmental and health externalities. Dialogues between developed and developing economies should be initiated so that all the stakeholders can seek potential solutions through integrated efforts.

Fostering sustainable supply chains is another key measure to ensure the co-achievement of SDG8, SDG10, and SDG13[63]. In many developing economies, weak workplace safety regulations leave workers exposed to climate-related hazards, especially in sectors like agriculture and manufacturing that are critical for trade. Profit-driven supply chains may "race to the bottom" by outsourcing production to regions with the least regulations and lowest labour costs, thereby exacerbating the risks for workers. Therefore, it is crucial to establish global standards that protect workers' rights and safety. Such measures not only safeguard the labour force but also contribute to the broader goals of decent work, reducing inequalities, and combating climate change.

Methods
Analytical framework
This study uses a multi-regional input-output model with a labour satellite account to estimate labour hours embodied in the global production networks, which is further combined with the gridded population to obtain grid-level labour in production networks. By combining
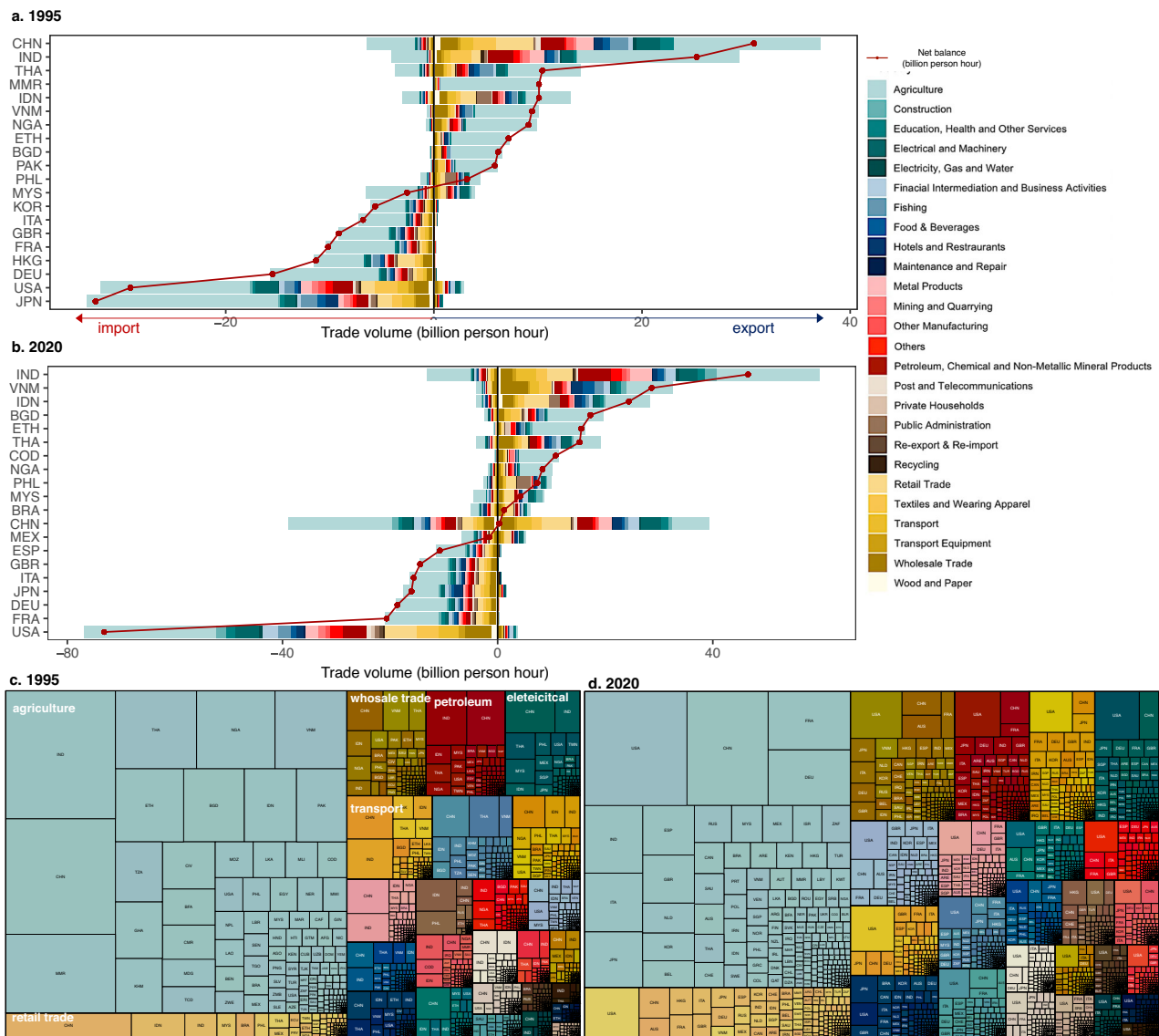
Fig. 5 | Exposure embodied in trade by economy and sector. a, b Exposure embodied in exports and imports for the top twenty economies with the largest exposure trading volume in 1995 and 2020. The connected red dots show the net exposure balance. **c, d** Exposure embodied in global exports by sector and economy in 1995 and 2020 on the production side. Source data are provided as a Source Data file.

this with a climate model that provides grid-level heat exposure, as well as with other data such as average working hours, labour's exposure to heat stress can be accounted for. How these modules are integrated is illustrated in Supplementary Information (Supplementary Figs. 1, 2).

Labour embodied in trade

The input-output (IO) model has been widely adopted to investigate the interconnections between different sectors. By applying multi-regional input-output (MRIO) models, researchers can uncover how countries/regions are connected bilaterally through trade. These MRIO models can be extended with satellite accounts to trace emissions, resources, pollution, water, land, as well as many other aspects transferred through the international production system[42,64,65]. Here, we use a global multi-regional input-output model to trace labour hours embodied in trade. Assuming that there are m regions and n sectors involved in international trade, the equilibrium between product supply and demand can be expressed in Eq. (1).

$$AX + Y = X \tag{1}$$

where, **A** is a direct input coefficient matrix, **X** is the total output matrix, and **Y** is the final demand matrix. The Leontief model links final demand with gross outputs, which is shown in Eq. (2).

$$X = (I - A)^{-1}Y = BY \tag{2}$$

where **B** is the Leontief inverse matrix. Denote the labour intensity matrix by **E**, which is a diagonalized matrix representing labour employment per unit of gross output for each region-sector, we can get Eq. (3).

$$L = EBY \tag{3}$$

$\mathbf{L}_{mn \times mn}$ is the global labour employed, in which its element l_{isjr} is the labour employment in region i sector s created by region j sector r. Thus, by summing the matrix **L** by rows, we obtain production side labour employment of each region-sector; summing the matrix **L** by columns, we obtain consumption side labour induced by each region-sector.

Matching labour employment data to MRIO

There are 26 sectors in the Eora multiregional input-output tables, and 14 economic activities in the International Labour Organisation (ILO) labour employment database. To match the labour employment categories with Eora economic sectors we follow a widely adopted approach, namely matching these two data sources by using a concordance table (Supplementary Table 2).

Measuring extreme heat exposure hours

To measure labour force exposure hours to extreme heat, we combine climate models with socio-economic information. The climate model is based on the ERA5[66], from which researchers have developed the universal thermal climate index (UTCI)[36]. UTCI is a human biometeorology parameter—an equivalent temperature (°C)—that measures human physiological response to the thermal environment. By considering how the human body experiences atmospheric conditions (air temperature, humidity, wind, and radiation), the UTCI describes synergistic heat exchanges between the thermal environment and the human body. Four variables from the ERA5 are necessary to build the UTCI index, including 2 m air temperature, 2 m dew point temperature (or relative humidity), wind speed at 10 m above the ground level and mean radiant temperature (MRT). There are 10 UTCI thermal stress categories that correspond to specific human physiological responses to the thermal environment. The categories related to UTCI degree Celsius (°C) are as follows: above +46: extreme heat stress; + 38 to + 46: very strong heat stress; + 32 to + 38: strong heat stress; + 26 to + 32: moderate heat stress; + 9 to + 26: no thermal stress; + 9 to 0: slight cold stress; 0 to − 13: moderate cold stress; − 13 to − 27: strong cold stress; − 27 to − 40: very strong cold stress; below − 40: extreme cold stress (Supplementary Table 3). Thus, working hours each day can be classified into different heat stress levels (Supplementary Figs. 35–222). Defining the exposure to heat exposure as the number of hours exposed to extreme/very strong/strong heat stress, the UTCI index can be converted to a binary heat exposure indicator, which is shown in Eq. (4).

$$H_{gydh} = \begin{cases} 0, \text{UTCI}^c_{gydh} < 32 \\ 1, \text{UTCI}^c_{gydh} \geq 32 \end{cases} \tag{4}$$

where UTCI^c_{gydh} is the converted UTCI index for the gth grid on hour h in day d of year y, by subtracting 273.15 from the original UTCI index stored in Kelvin (K). Then we make two assumptions. First, following the idea of 12 h exposure time in previous studies, we set the maximum daily working hour to be 12 h, which is equivalent to 2400 annual working hours for 200 work days/year and 3000 annual working hours for 250 work days/year. Second, as different grids may differ in annual work hours and average daily work hours, we assume that the annual work hours are evenly distributed throughout the 12 h available work time per day. Then, the daily and annual heat exposure cap can be summed by using Eq. (5).

$$H_{gyd} = \begin{cases} \sum_h H_{gydh}, & \sum_h H_{gydh} \leq 12 \\ 12, & \sum_h H_{gydh} > 12 \end{cases}, \quad H_{gy} = \sum_d H_{gyd} \tag{5}$$

Thus, the average exposed work hours to heat can be obtained by using Eq. (6).

$$w_{gy} = H_{gy} \times \frac{\omega_{gy}}{12 \times 365} \tag{6}$$

where ω_{gy} is the average work hours of the labour force in gth grid for year y, which is obtained from region-specific database and estimation.

Linking grid cell labour embodied with grid cell exposure

We use a population density module to link the interregional embodied labour flow with grid cell annual average per capita work hours

exposed to extreme heat. Thus, the labour force within each grid cell can be linked from a production network perspective, which is shown in Eq. (7).

$$l_{gsjr} = l_{isjr} \times \frac{p_{gy} \times a_g}{\sum_{g \in G_i} p_{gy} \times a_g} \tag{7}$$

where p_{gy} is the population density of the gth grid in year y, a_g is the area of the gth grid, and G_i is all grid cells in country/region i. Then the labour force exposure to extreme temperatures (LET) linked with the production network on the grid cell level and country/region level can be expressed in Eqs. (8, 9).

$$\text{LET}_{gsjr} = w_{gy} \times l_{isjr} \times \frac{p_{gy} \times a_g}{\sum_{g \in G_i} p_{gy} \times a_g} \tag{8}$$

$$\text{LET}_{isjr} = \sum_{g \in G_i} w_{gy} \times l_{isjr} \times \frac{p_{gy} \times a_g}{\sum_{g \in G_i} p_{gy} \times a_g} = l_{isjr} \times \frac{\sum_{g \in G_i} w_{gy} \times p_{gy} \times a_g}{\sum_{g \in G_i} p_{gy} \times a_g} \tag{9}$$

Here, LET_{isjr} represents the embodied heat exposure of the labour force, l_{isjr} represents the embodied labour employment, and $\frac{\sum_{g \in G_i} w_{gy} \times p_{gy} \times a_g}{\sum_{g \in G_i} p_{gy} \times a_g}$ reflects the average per capita exposure. Summing LET by i and s, we obtain the total heat exposure induced by sector r in region j, which is a consumption side exposure; while summing LET by j and r, we obtain the total heat exposure induced by sector s in region i, which is a production side exposure.

Structural decomposition analysis

We use an SDA to attribute the role of each driving factor in the total changes in labour force heat exposure (Supplementary Method 1). Based on Eqs. (3) and (9), we quantify **LET** based on the input-output framework in a matrix form,

$$\textbf{LET} = \textbf{HEBY}_s \textbf{Y}_t \tag{10}$$

where **H** is the diagonal matrix for average heat exposure index per labour employed in each country, **E** is a diagonal matrix for labour intensity per gross output for each country-sector, **B** is the Leontief inverse matrix representing the production structure, $\textbf{Y}_s$ is a $mn \times m$ matrix with the sum of all elements equal to 1, representing the final demand structure, and $\textbf{Y}_t$ is the diagonal matrix with all diagonal elements as the same value—the deflated global total demand. Thus, the changes **LET** can be attributable to its driving factors, including the climate change effect $\Delta\textbf{H}$, the labour intensity effect $\Delta\textbf{E}$, the production structure effect $\Delta\textbf{B} = \Delta\textbf{B}^d + \Delta\textbf{B}^e$, the final demand structure effect $\Delta\textbf{Y}_s = \Delta\textbf{Y}_s^d + \textbf{Y}_s^e$, and the total final demand growth effect $\Delta\textbf{Y}_t$,

$$\Delta\textbf{LET} = \Delta\textbf{H} + \Delta\textbf{E} + \Delta\textbf{B} + \Delta\textbf{Y}_s + \Delta\textbf{Y}_t \tag{11}$$

Then, we apply the SDA method on constant price input-output tables obtained by taking the Producer Price Indices (PPIs) as deflators and the Logarithmic Mean Divisia Index (LMDI) approach to estimate the role of each driving factor between time periods (Supplementary Fig. 7).

Robustness analysis

To test the robustness of the results, this study further conducts several sensitivity analyses. First, a comparison between this study and previous studies was conducted (Supplementary Table 4). Second, we use alternative data sources by replacing the input-output table from Eora with Inter-Country Input-Output tables compiled by the

Organisation for Economic Co-operation and Development (OECD-ICIO), which consists of 67 economies and 45 sectors from 1995 to 2018. The results drawn from these two data sources are compared on the global and national levels both on the production and consumption sides from 1995 to 2015 (Supplementary Figs. 223–225). Third, we also use Monte Carlo simulation to test the robustness of the original heat exposure estimation, based on whether it falls within the expected range of values derived from the simulations. We conduct 1000 Monte Carlo simulations, where the heat stress drawn from the ERA5 is set to a normal distribution with a mean equal to the baseline values and a standard deviation set to 10% of each respective baseline value. The results indicate that the original estimation falls well within the range of expected values generated by these simulations, and the global labour force's total heat exposure remain robust from 1995 to 2020 when heat stress varies within an acceptable level (Supplementary Figs. 226–228).

Data

Multiregional Input-output tables. To measure trade flows between countries/regions, we need to use information from MRIO tables. There are several available MRIO databases, including Eora[67], World Input-Output Database (WIOD)[68], OECD-ICIO[69], and Exiobase[70], as well as other newly emerging databases. In this study, the global MRIO table is collected from the Eora global supply chain database. Eora provides high-resolution multiregional IO tables with matching environmental and social satellite accounts for 190 economies and 26 sectors. Its full geographical coverage, especially with detailed information on tropical and low-income economies, allows all the global labour employment to be analysed. In addition, it has a long temporal coverage, which helps uncover the trends and compare them across different time periods.

Labour employment. Labour employment data were drawn from the International Labour Organisation (ILO) via ILOSTAT explorer. The ILO-modelled estimates provide a complete set of internationally comparable labour statistics, which is a balanced panel data set with consistent country/region coverage. The data is mainly based on nationally reported observations, and the missing data is imputed using the ILO model. ILO evaluates existing self-reported data, selects only those observations deemed sufficiently comparable across countries/regions and runs the model to obtain the ILO-modelled estimates. For the working-age population who is at least 15 years old, the labour employment data from ILO provides a breakdown of total employment by economic sector and gender. The economic activity classification is based on the International Standard Industrial Classification (ISIC) Rev.4, which includes 14 sectors.

Working Hours. The average number of annual working hours for the labour force in each country/region is originally obtained from Penn World Table version 10.01. Penn World Table is a database with information on relative levels of income, output, input and productivity, covering 183 countries/regions between 1950 and 2019[41]. We use variable *avh* in the database—average annual work hours by labour engaged—as the work hours for each country/region. For those countries that have missing data for a given year, we use the random forest to fill in the missing values (Supplementary Method 2 and Supplementary Fig. 229). For the year 2020, the relevant data from 2019 was applied in the analysis.

Gridded population density data. To capture heterogeneous levels of exposure to extreme heat geographically, we need to split those country-level employment data to the grid level. To do this, we use the population density in each grid from the fourth version of the Gridded Population of the World data (GPWv4). In GPWv4, population input data were collected at the detailed spatial resolution available from the results of the 2010 round of Population and Housing Censuses and then extrapolated to produce population estimates for years 2000, 2005, 2010, 2015, and 2020. For the year 1995, which is not covered by GPWv4, the population density of the year 2000 is used instead. The population density raster data sets are gridded with an output resolution of 30 arc-seconds (~1 km at the equator).

Climate data. To obtain gridded extreme heat exposure, we draw climate data from the ECMWF ERA5 reanalysis. The ERA5 provides UTCI —an equivalent temperature that measures human physiological response to the thermal environment. To obtain the daily extreme heat hours in each grid, we separate the UTCI index by categories: (1) above +46: extreme heat stress; (2) +38 to +46: very strong heat stress; (3) +32 to +38: strong heat stress; (4) +26 to +32: moderate heat stress; (5) +9 to +26: no thermal stress; (6) +9 to 0: slight cold stress; (7) 0 to −13: moderate cold stress; (8) −13 to −27: (9) strong cold stress; (10) −27 to −40: very strong cold stress; below −40: extreme cold stress.

Reporting summary

Data availability

Multiregional input-output tables were collected from the Eora global supply chain database, which is accessible on https://worldmrio.com with a valid license. Labour employment data were drawn from ILO. The data for labour employment can be accessed at https://webapps. ilo.org/ilostat-files/WEB_bulk_download/html/bulk_indicator.html. The average annual work hours in different countries were obtained from the Penn World Table (version 10.01). The Penn World Table can be accessed at https://dataverse.nl/dataset.xhtml?persistentId=doi:10. 34894/QT5BCC. Climate data and gridded extreme heat exposure data were drawn from the ECMWF ERA5 reanalysis. The ERA5 data can be accessed at https://climate-adapt.eea.europa.eu/en/metadata/ indicators/thermal-comfort-indices-universal-thermal-climate-index-1979-2019). Gridded population density data were obtained from GPWv4. The GPWv4 data can be accessed at https://sedac.ciesin. columbia.edu/data/collection/gpw-v4. The country boundaries data is from Esri, Garmin International, the US Central Intelligence Agency, and the National Geographic Society. World Countries (Generalised). The country boundaries data was downloaded from https://hub.arcgis. com/datasets/esri::world-countries-generalized. The data generated in this study are provided in the Source Data file. Source data are provided in this paper.

Code availability

The code necessary to replicate this study can be accessed at Figshare (https://doi.org/10.6084/m9.figshare.25624338.v1).

References

1. Schiermeier, Q. Climate change made North America's deadly heatwave 150 times more likely. *Nature* https://doi.org/10.1038/ d41586-021-01869-0 (2021).
2. Vicedo-Cabrera, A. M. et al. The burden of heat-related mortality attributable to recent human-induced climate change. *Nat. Clim. Change* **11**, 492–500 (2021).
3. Perkins-Kirkpatrick, S. E. & Lewis, S. C. Increasing trends in regional heatwaves. *Nat. Commun.* **11**, 3357 (2020).
4. Pennisi, E. Living with heat. *Science* **370**, 778–781 (2020).
5. United Nations Office for Disaster Risk Reduction. *The Human Cost of Disasters: An Overview of the Last 20 Years (2000–2019)*. http:// www.undrr.org/quick/50922 (2020).
6. Mora, C. et al. Global risk of deadly heat. *Nat. Clim. Change* **7**, 501–506 (2017).
7. Schär, C. et al. The role of increasing temperature variability in European summer heatwaves. *Nature* **427**, 332–336 (2004).
8. Barriopedro, D., Fischer, E. M., Luterbacher, J., Trigo, R. M. & García-Herrera, R. The hot summer of 2010: redrawing the temperature record map of Europe. *Science* **332**, 220–224 (2011).

9. Kjellstrom, T., Freyberg, C., Lemke, B., Otto, M. & Briggs, D. Estimating population heat exposure and impacts on working people in conjunction with climate change. *Int. J. Biometeorol.* **62**, 291–306 (2018).

10. Flouris, A. D. et al. Workers' health and productivity under occupational heat strain: a systematic review and meta-analysis. *Lancet Planet. Health* **2**, e521–e531 (2018).

11. International Labour Office. *Working on a Warmer Planet: The Impact of Heat Stress on Labour Productivity and Decent Work*. (2019).

12. Autor, D. H., Dorn, D. & Hanson, G. H. The China syndrome: Local labor market effects of import competition in the United States. *Am. Econom. Rev.* **103**, 2121–2168 (2013).

13. OECD. *Global Value Chains and Trade in Value-Added: An Initial Assessment of the Impact on Jobs and Productivity*. https://www.oecd-ilibrary.org/trade/global-value-chains-and-trade-in-value-added-an-initial-assessment-of-the-impact-on-jobs-and-productivity_5jlvc7sb5s8w-en (2016).

14. Tzachor, A. et al. How to reduce Africa's undue exposure to climate risks. *Nature* **620**, 488–491 (2023).

15. Ebi, K. L. et al. Hot weather and heat extremes: health risks. *Lancet* **398**, 698–708 (2021).

16. Watts, N. et al. The 2020 report of The Lancet Countdown on health and climate change: responding to converging crises. *Lancet* **397**, 129–170 (2021).

17. Mazdiyasni, O. et al. Increasing probability of mortality during Indian heat waves. *Sci. Adv.* **3**, e1700066 (2017).

18. Matthews, T. K. R., Wilby, R. L. & Murphy, C. Communicating the deadly consequences of global warming for human heat stress. *Proc. Natl. Acad. Sci. USA* **114**, 3861–3866 (2017).

19. Kjellstrom, T., Lemke, B. & Lee, J. Workplace Heat: An increasing threat to occupational health and productivity. *Am. J. Ind. Med.* **62**, 1076–1078 (2019).

20. Liu, M., Shamdasani, Y. & Taraz, V. Climate change and labor reallocation: Evidence from six decades of the Indian census. *Am. Econ. J. Econ. Polic.* **15**, 395–423 (2023).

21. Jay, O. & Kenny, G. P. Heat exposure in the Canadian workplace. *Am. J. Ind. Med.* **53**, 842–853 (2010).

22. Kong, Q. & Huber, M. Explicit Calculations of Wet-Bulb Globe Temperature Compared With Approximations and Why It Matters for Labor Productivity. *Earth's Future* **10**, https://doi.org/10.1029/2021EF002334 (2022).

23. Zander, K. K., Botzen, W. J. W., Oppermann, E., Kjellstrom, T. & Garnett, S. T. Heat stress causes substantial labour productivity loss in Australia. *Nat. Clim. Change* **5**, 647–651 (2015).

24. Burke, M., Hsiang, S. M. & Miguel, E. Global non-linear effect of temperature on economic production. *Nature* **527**, 235–239 (2015).

25. Orlov, A., Sillmann, J., Aunan, K., Kjellstrom, T. & Aaheim, A. Economic costs of heat-induced reductions in worker productivity due to global warming. *Glob. Environ. Change* **63**, 102087 (2020).

26. García-León, D. et al. Current and projected regional economic impacts of heatwaves in Europe. *Nat. Commun.* **12**, 5807 (2021).

27. Ballester, J. et al. Heat-related mortality in Europe during the summer of 2022. *Nat. Med.* **29**, 1857–1866 (2023).

28. Barreca, A., Clay, K., Deschênes, O., Greenstone, M. & Shapiro, J. S. Convergence in Adaptation to Climate Change: Evidence from High Temperatures and Mortality, 1900–2004. *Am. Econ. Rev.* **105**, 247–251 (2015).

29. Barreca, A., Clay, K., Deschenes, O., Greenstone, M. & Shapiro, J. S. Adapting to climate change: The remarkable decline in the US temperature-mortality relationship over the twentieth century. *J. Political Econ.* **124**, 105–159 (2016).

30. Sun, S. et al. Ambient heat and risks of emergency department visits among adults in the United States: time stratified case crossover study. *BMJ* **375**, https://doi.org/10.1136/bmj-2021-065653 (2021).

31. Russo, S. et al. Half a degree and rapid socioeconomic development matter for heatwave risk. *Nat. Commun.* **10**, 136 (2019).

32. Lüthi, S. et al. Rapid increase in the risk of heat-related mortality. *Nat. Commun.* **14**, 4894 (2023).

33. Sun, Y. et al. Global supply chains amplify economic costs of future extreme heat risk. *Nature* **627**, 797–804 (2024).

34. Zhang, Z., Zhang, W., Wu, Q., Liu, J. & Jiang, L. Do heat waves melt away imports: Evidence and mechanisms from China. *China Econ. Rev.* **84**, 102133 (2024).

35. Knittel, N., Jury, M. W., Bednar-Friedl, B., Bachner, G. & Steiner, A. K. A global analysis of heat-related labour productivity losses under climate change—implications for Germany's foreign trade. *Clim. Change* **160**, 251–269 (2020).

36. Di Napoli, C., Barnard, C., Prudhomme, C., Cloke, H. L. & Pappenberger, F. ERA5-HEAT: A global gridded historical dataset of human thermal comfort indices from climate reanalysis. *Geosci. Data J.* **8**, 2–10 (2021).

37. World Bank Country and Lending Groups – World Bank Data Help Desk. https://datahelpdesk.worldbank.org/knowledgebase/articles/906519-world-bank-country-and-lending-groups. (2024).

38. Friedlingstein, P. et al. Global Carbon Budget 2023. *Earth Syst. Sci. Data* **15**, 5301–5369 (2023).

39. Andrew, R. M. & Peters, G. P. The Global Carbon Project's fossil CO2 emissions dataset. Zenodo https://doi.org/10.5281/zenodo.10177738 (2023).

40. Chen, X., Li, N. & Jiang, D. Global and regional changes in working-age population exposure to heat extremes under climate change. *J. Geogr. Sci.* **33**, 1877–1896 (2023).

41. Feenstra, R. C., Inklaar, R. & Timmer, M. P. The next Generation of the Penn World Table. *Am. Econ. Rev.* **105**, 3150–3182 (2015).

42. Meng, B. et al. Developing countries' responsibilities for CO2 emissions in value chains are larger and growing faster than those of developed countries. *One Earth* **6**, 167–181 (2023).

43. Hoekstra, R., Michel, B. & Suh, S. The emission cost of international sourcing: using structural decomposition analysis to calculate the contribution of international sourcing to CO_2-emission growth. *Econ. Syst. Res.* **28**, 151–167 (2016).

44. Broadbent, A. M., Krayenhoff, E. S. & Georgescu, M. The motley drivers of heat and cold exposure in 21st century US cities. *Proc. Natl. Acad. Sci. USA* **117**, 21108–21117 (2020).

45. Georgescu, M., Broadbent, A. M. & Krayenhoff, E. S. Quantifying the decrease in heat exposure through adaptation and mitigation in twenty-first-century US cities. *Nat. Cities* **1**, 42–50 (2023).

46. Lenton, T. M. et al. Quantifying the human cost of global warming. *Nat. Sustain.* **6**, 1237–1247 (2023).

47. Tuholske, C. et al. Global urban population exposure to extreme heat. *Proc. Natl. Acad. Sci. USA* **118**, e2024792118 (2021).

48. Jones, B. et al. Future population exposure to US heat extremes. *Nat. Clim. Change* **5**, 652–655 (2015).

49. Hoogeveen, J., Tesliuc, E. & Vakis, R. A Guide to the Analysis of Risk, Vulnerability and Vulnerable Groups. *Policy Research Working Paper*, World Bank. (2004).

50. Diffenbaugh, N. S. & Burke, M. Global warming has increased global economic inequality. *Proc. Natl. Acad. Sci. USA* **116**, 9808–9813 (2019).

51. Kjellstrom, T., Holmer, I. & Lemke, B. Workplace heat stress, health and productivity – an increasing challenge for low and middle-income countries during climate change. *Glob. Health Action* **2**, 2047 (2009).

52. Hsiang, S. et al. Estimating economic damage from climate change in the United States. *Science* **356**, 1362–1369 (2017).

53. Kephart, J. L. et al. City-level impact of extreme temperatures and mortality in Latin America. *Nat. Med.* **28**, 1700–1705 (2022).

54. Callahan, C. W. & Mankin, J. S. Globally unequal effect of extreme heat on economic growth. *Sci. Adv.* **8**, eadd3726 (2022).

55. Harrington, L. J. et al. Poorest countries experience earlier anthropogenic emergence of daily temperature extremes. *Environ. Res. Lett.* **11**, 055007 (2016).

56. Thompson, V. et al. The most at-risk regions in the world for high-impact heatwaves. *Nat. Commun.* **14**, 2152 (2023).

57. ILO and UNICEF. *Child Labour: Global Estimates 2020, Trends and the Road Forward*. (2021).

58. Parsons, L. A., Shindell, D., Tigchelaar, M., Zhang, Y. & Spector, J. T. Increased labor losses and decreased adaptation potential in a warmer world. *Nat. Commun.* **12**, 7286 (2021).

59. Lesnikowski, A., Ford, J., Biesbroek, R., Berrang-Ford, L. & Heymann, S. J. National-level progress on adaptation. *Nat. Clim. Change* **6**, 261–264 (2016).

60. Kjellstrom, T., Kovats, R. S., Lloyd, S. J., Holt, T. & Tol, R. S. J. The direct impact of climate change on regional labor productivity. *Arch. Environ. Occup. Health* **64**, 217–227 (2009).

61. Dunne, J. P., Stouffer, R. J. & John, J. G. Reductions in labour capacity from heat stress under climate warming. *Nat. Clim. Change* **3**, 563–566 (2013).

62. Fankhauser, S. & McDermott, T. K. J. Understanding the adaptation deficit: Why are poor countries more vulnerable to climate events than rich countries? *Glob. Environ. Change* **27**, 9–18 (2014).

63. Yan, L. Supply-chain adaptation. *Nat. Clim. Chang.* **14**, 117–117 (2024).

64. Peters, G. P. & Hertwich, E. G. CO2 Embodied in international trade with implications for global climate policy. *Environ. Sci. Technol.* **42**, 1401–1407 (2008).

65. Lenzen, M. et al. Implementing the material footprint to measure progress towards Sustainable Development Goals 8 and 12. *Nat. Sustain.* **5**, 157–166 (2022).

66. Hersbach, H. et al. The ERA5 global reanalysis. *Q. J. R. Meteorol. Soc.* **146**, 1999–2049 (2020).

67. Lenzen, M., Moran, D., Kanemoto, K. & Geschke, A. BUILDING EORA: A GLOBAL MULTI-REGION INPUT–OUTPUT DATABASE AT HIGH COUNTRY AND SECTOR RESOLUTION. *Econ. Syst. Res.* **25**, 20–49 (2013).

68. Dietzenbacher, E., Los, B., Stehrer, R., Timmer, M. & De Vries, G. The construction of world input–output tables in the WIOD project. *Econ. Syst. Res.* **25**, 71–98 (2013).

69. OECD. OECD Inter-Country Input-Output (ICIO) Tables. https://www.oecd.org/sti/ind/inter-country-input-output-tables.htm (2021).

70. Giljum, S. et al. The impacts of data deviations between MRIO models on material footprints: A comparison of EXIOBASE, Eora, and ICIO. *J. Ind. Ecol.* **23**, 946–958 (2019).

Author contributions

M.L., B.M., and Y.G. designed the research. M.L. determined the methods and carried out the calculation and analysis. N.Y. contributed to the data. B.M., F.T., YN.G., N.Y., S.L., J.G., and K.U. improved the analysis and the figures. M.L., B.M., and Y.G. wrote the manuscript. M.L., Y.G., F.T., S.L., and X.C. revised the manuscript. Y.G. refers to Yong Geng. YN.G. refers to Yuning Gao.

Competing interests

The authors declare no competing interests.

Additional information

Supplementary information The online version contains supplementary material available at https://doi.org/10.1038/s41467-024-55483-5.

Correspondence and requests for materials should be addressed to Bo Meng or Yong Geng.

Peer review information *Nature Communications* thanks Nina Knittel, Sangwon Suh, and XIANCHUN TAN for their contribution to the peer review of this work. A peer review file is available.

Reprints and permissions information is available at http://www.nature.com/reprints

Publisher's note Springer Nature remains neutral with regard to jurisdictional claims in published maps and institutional affiliations.